

Supplementary Materials

S1. POPC sensibility to aerosol composition

The POPC size thresholds are determined using known PolyStyrene Latex (PSL) particles. Figure S1 shows the scattering efficiency for individual particles derived from Mie calculations (Hagan et al., 2022) for PSL, sulfate (70% H_2SO_4 /30% H_2O) (Knepf et al., 2024), and sea salt (Bi et al., 2018) by accounting for the physical parameters of the POPC such as laser wavelength, detector position, size thresholds (Vernier et al., 2025, in preparation). The scattering efficiency for both sea salt and sulfate are systematically lower than PSL and therefore the size of the POPC within the HTHH plume is underestimated. A correction factor was applied to the size threshold of the POPC to account for the lower scattering efficiency of particles that may have been present in the HTHH plume compared to the PSL particles.

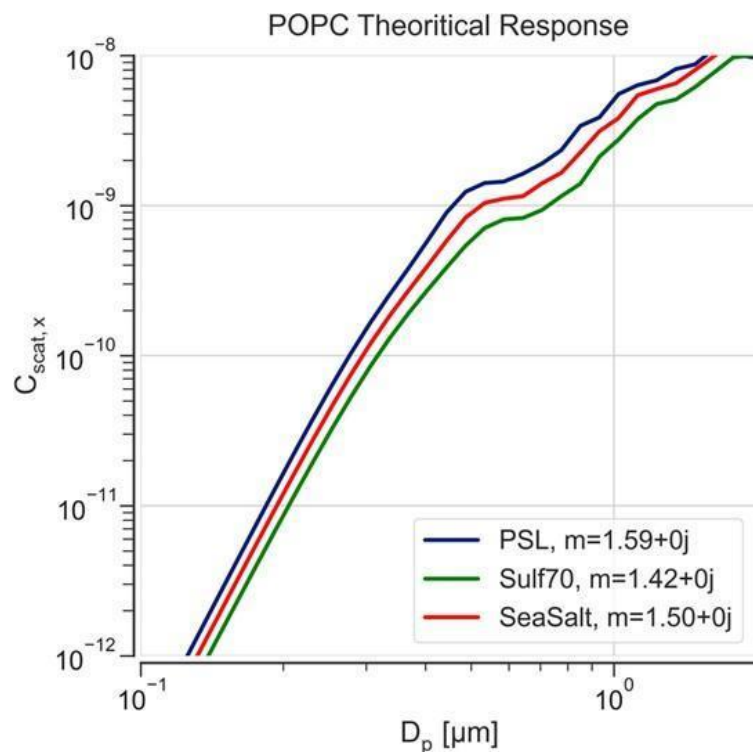


Fig. S1: Mean Scattering Efficiency for three different types of particles (PSL, Sulfate, Sea Salt) near 785 nm.

S2. Comparison between POPC, SAGE and COBALD

The systematic lower scattering efficiency of sulfate and sea salt led us to test how the assumption on composition could affect the retrieved extinction profiles compared to SAGE III/ISS and COBALD. The balloon flight with POPC and COBALD was launched to coincide with a SAGE III/ISS occultation measurement performed within a 300 km radius and a 2-hr window on 08/12/2022. Fig. S2 includes collocated extinction profiles from the Stratospheric Aerosol and Gas Experiment (SAGE) III along with balloon data (COBALD and POPC). POPC extinction profiles were calculated using composition-based correction factors, log-normal distribution fitting, and Mie theory at various wavelengths. The assumption of sulfate (RI=1.42) or sea salt (RI=1.50) aerosol composition yielded better agreement between SAGE III/ISS, COBALD, and POPC data across the 455-1020 nm spectral range.

The corrections improved the comparison between SAGE III/COBALD and POPC between 18 and 26 km within the Hunga plume. Assuming sea salt improves especially the extinction profile at 1022 nm, which becomes, for most of the profile, within +/- 50% from SAGE III. SAGE III and OPC measurements over Laramie were within +/-40% for most of the cases in background conditions (Deshler,T. et al., 2003). Obtaining such an agreement with the POPC within the HTHH plume indicates the robustness of the POPC measurements in volcanically perturbed conditions. Table 3 provides a summary of the overall comparison after calculating the SAOD from the tropopause to 40 km. While the sea salt assumption tends to improve the comparison in the near infrared part of the spectrum, the sulfate assumption seems better in the visible. Given the similar optical properties of sea salt and sulfate, the comparison remains inconclusive regarding the composition of the plume we can derive from this comparison and therefore we cannot rule out the presence of sea salt-like aerosols in the HTHH plume.

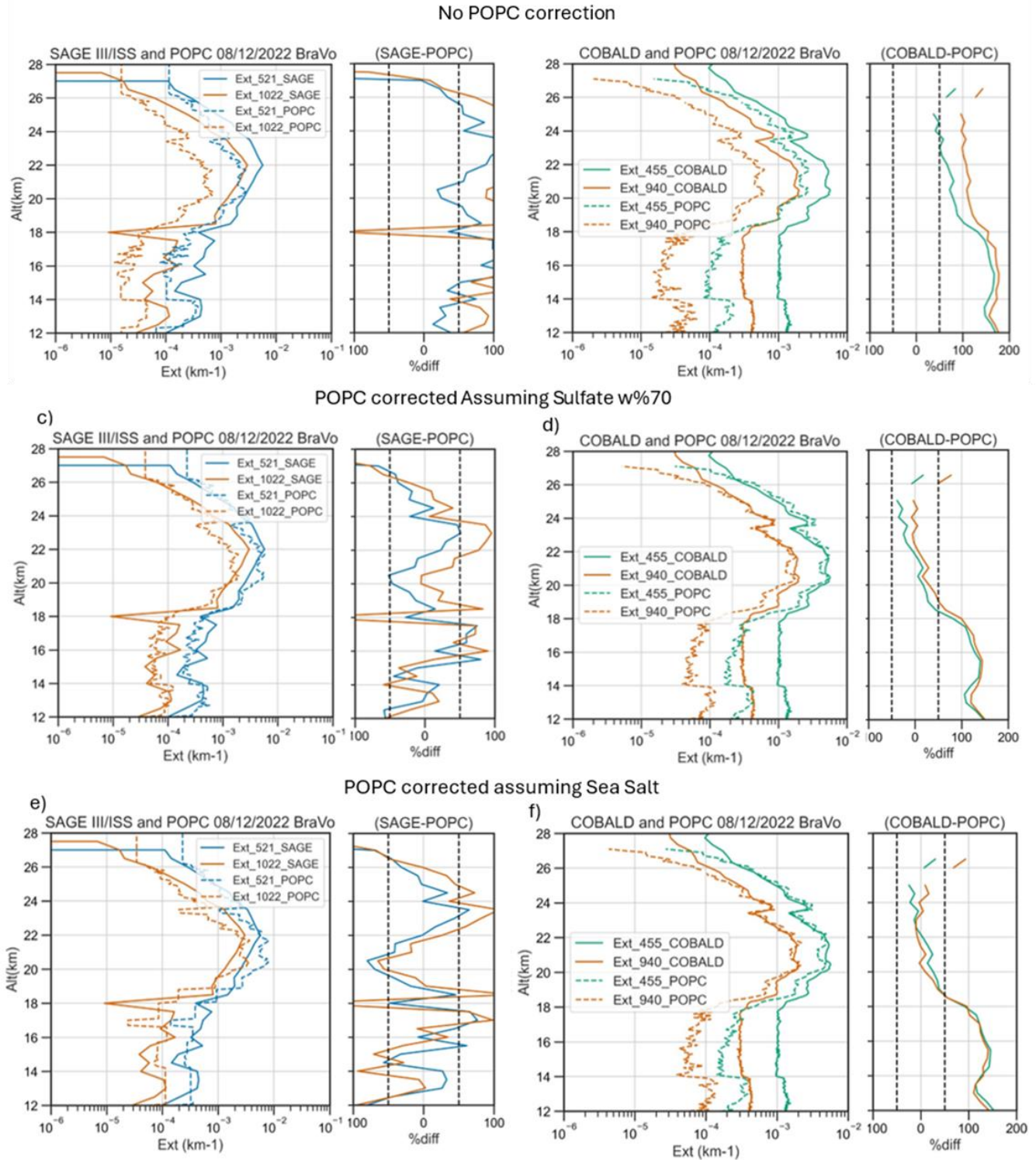


Figure S2: POPC-derived, SAGE III/ISS, and COBALD Extinction profiles on 08/12. a) &b) no correction, c) & d) size corrected assuming sulfate refractive index=1.42, e) & f) assuming sea salt refractive index=1.50. The POPC data fitted with a lognormal distribution before deriving the extinction values

Table.S1 Comparison between SAOD at different wavelengths (column 1; line 1-4) calculated from POPC without (column “POPC”) corrections assuming either sea salt (column “POPC_SeaSalt”) or Sulfate (column “POPC_Sul70”). In brackets are the percentage difference with either SAGE III or COBALD SAOD.

Variables	Sampler	SAGE III	COBALD	POPC	POPC_Sul70	POPC_SeaSalt
SAOD_521	x	0.022	x	0.011(-50%)	0.023(4%)	0.027(18%)
SAOD_1022	x	0.010	x	0.002(-80%)	0.007(-0%)	0.010(0%)
SAOD_455	x	x	0.025	0.011(-56%)	0.023(-8%)	0.021(-16%)
SAOD_940	x	x	0.008	0.002	0.007(-12%)	0.008(0%)

S3. Theoretical mass calculation from POPC measurements

Deriving aerosol mass from aerosol size distribution to simulate aerosol collection from the aerosol sampler requires several steps, which are described below:

Step 1: Analyze POPC data and fit a lognormal distribution to derive total concentration, mode radius, and standard deviation

Step 2: Use the distribution to calculate mass concentration as a function of altitude

Step 3: Use the sampler flow rate along the flight on 08/16 and calculate mass collected using 3 threshold size thresholds of $d > 0.01 \mu\text{m}$, $d > 0.3 \mu\text{m}$, and $d > 0.45 \mu\text{m}$

The aerosol size distribution derived from POPC measurements on 08/12 between 20-22 km is shown in Figure S3.

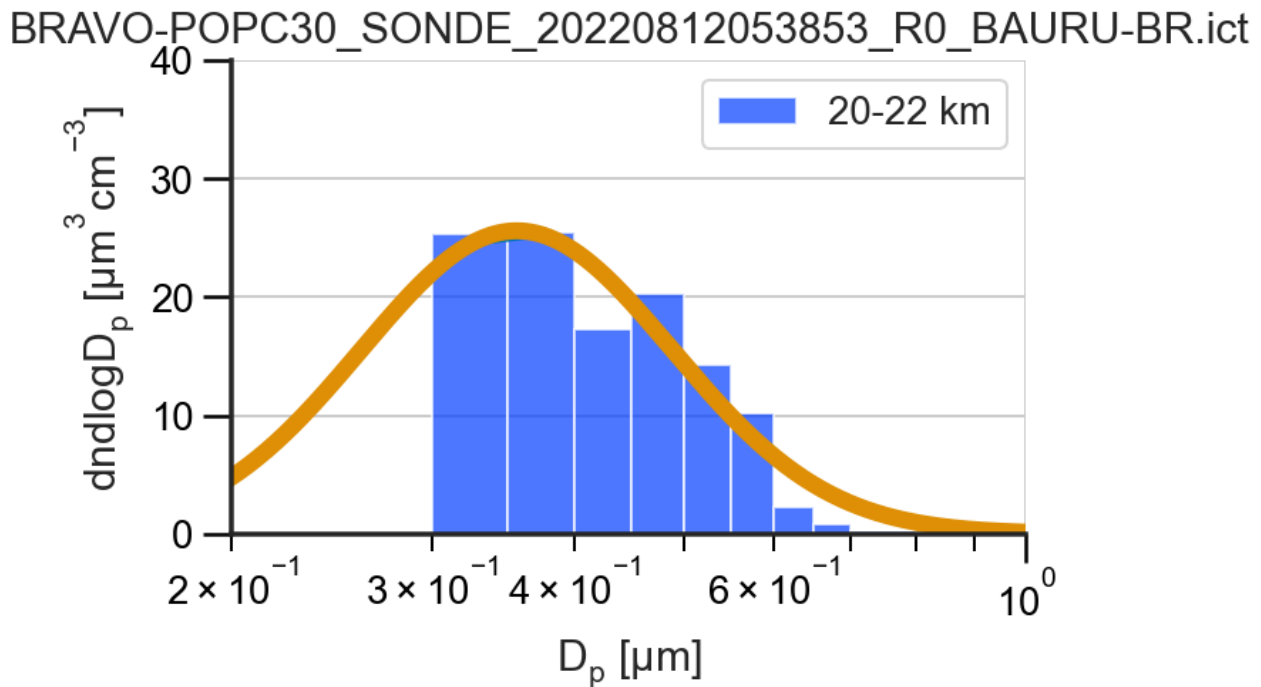


Figure S3. Number distribution function as defined in eq. 1 between 20-22 km on 08/12 based on POPC measurements. The orange line represents the lognormal fit of the distribution.

$$n_N^o(\log D_p) = \frac{dN}{d\log D_p} = \frac{N_t}{\sqrt{2\pi} \log \sigma_g} \exp\left(-\frac{(\log D_p - \log D_{pg})^2}{2 \log^2 \sigma_g}\right)$$

Eq. 1

where N is the number concentration, D_p is the median particle diameter (Geometric Mean), and σ_g is the standard deviation.

We used the opcsim library (<https://dhhagan.github.io/opcsim/>) to create Figure S3 and derived a lognormal fit to the aerosol size distribution. The total number concentration between two particle diameters is defined in Eq.2. Multiplied by the aerosol density assumed to be 1.8 kg/L, which corresponds to a mixture of 70% sulfuric acid and 30% water, consistent with stratospheric sulfate aerosol, the mass concentration can be derived.

$$N_t = \int_{D_{min}}^{D_{max}} n_N(D_p) dD_p$$

Eq. 2

Using the data of Fig. S3, we found the following results:

total mass con. $d>0.01\mu\text{m}$: $0.59\ \mu\text{g}/\text{m}^3$

total mass con. $d>0.3\ \mu\text{m}$: $0.55\ \mu\text{g}/\text{m}^3$

total mass con. $d>0.45\ \mu\text{m}$: $0.34\ \mu\text{g}/\text{m}^3$

total mass con. $d>0.6\ \mu\text{m}$: $0.14\ \mu\text{g}/\text{m}^3$

The following calculations aim to simplify estimates of mass collected by the aerosol sampler, assuming 40 min of float with the sampler and 2lpm \rightarrow total volume of air = 80 L $\rightarrow 0.08\ \text{m}^3$.

The results are shown below

total mass $d>0.01\mu\text{m}$:47 ng

total mass $d>0.3\mu\text{m}$: 44 ng

total mass $d>0.45\mu\text{m}$:27 ng

total mass $d>0.6\ \mu\text{m}$:11 ng

Therefore, a significant aerosol mass (~40%) could be lost depending on whether the pore size of the PTFE filters used ($0.45\mu\text{m}$) is considered as a threshold to calculate the total mass collected.

For Fig. 5c of the paper, the actual flow rate along the flight, together with the aerosol mass concentration from all three POPC flights, was used to calculate the theoretical mass calculated offering results comparable to those presented here with more simple calculations.

S4. ACE-FTS measurements

Satellite-based observations from the Atmospheric Composition Experiment-Fourier Transform Spectrometer (ACE-FTS) indicate the presence of sulfate aerosols in the HTHH plume. The nearest collocated profile, on August 15th near 24.3°S , 45°W , confirms this observation (Figure S4). The weight % ratio of $\text{H}_2\text{SO}_4/\text{H}_2\text{O}$ near 70% between 19-22 km and the large absorption dip near $1200\ \text{cm}^{-1}$ confirmed the presence of sulfate ions (Boone et al., 2022; Bernath et al., 2023) but those relative measurements do not allow the quantity of sulfate concentration. We investigated ACE-FTS from the time of the eruption to the BraVo campaign and found that the spectral signature was largely consistent with the presence of sulfate. However, the spectra over the first 2 months indicate that the dissolution of molecular H_2SO_4 into sulfate ions (SO_4^{2-}) appears to be slower than expected. Among other possibilities, the presence of NaCl could explain the lower dissociation rate (Eastes, J. W. (1989) but given the absence of spectral signature within the spectral windows of ACE-FTS, we cannot confirm the presence of NaCl . However, the early presence of NaCl in the plume would also be corroborated by the analysis of the samples collected after the eruption (Colombier et al., 2023) and explain the plume's early ozone depletion (Zhu et al., 2022; Evan et al., 2023).

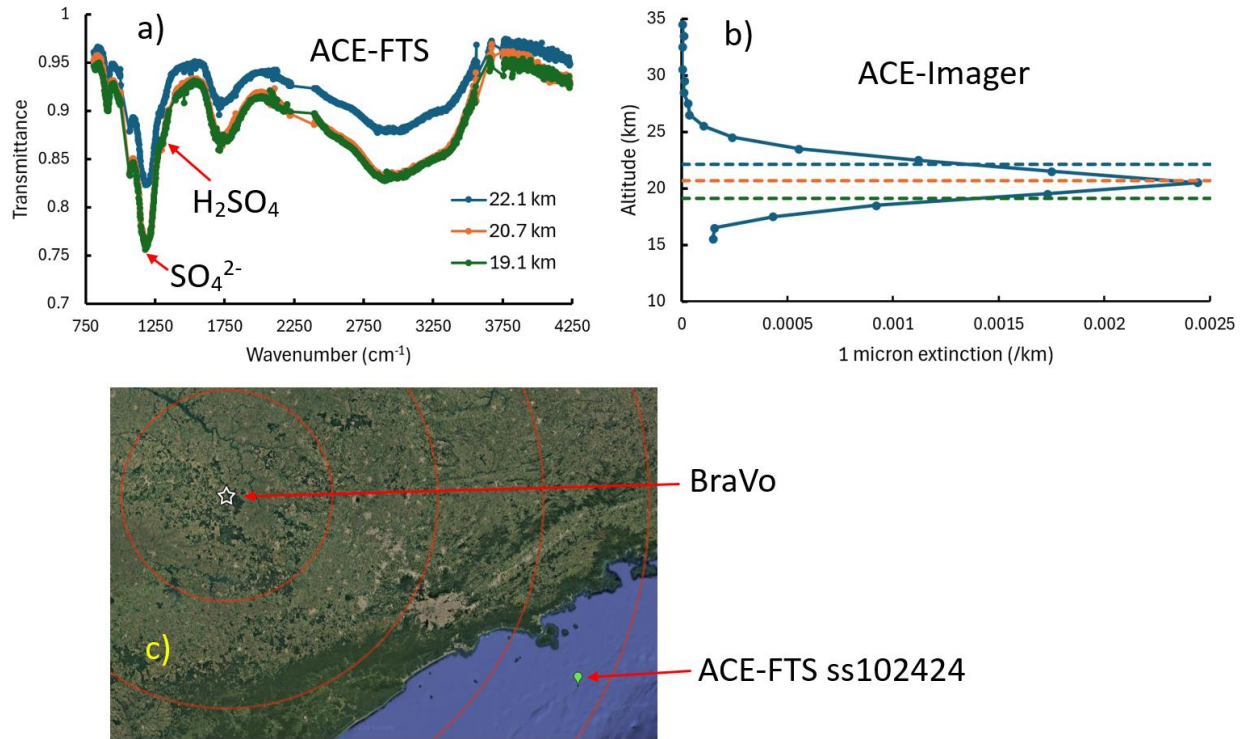


Figure S4. a) ACE-FTS spectra from ss102424, measured about 6 months following the Tonga eruption. b) corresponding extinction profile at 1 μm from Maestro on SciSat-1 satellite. c) the position of the measurements relative to the BraVo campaign is shown on the map.